# *Electronic Supplementary Information for*

# Electrostatically derived self-assembly of $NH_2$-mediated zirconium MOF with graphene for photocatalytic reduction of Cr(Ⅵ)

*Lijuan Shen,*[a] *Linjuan Huang,*[a] *Shijing Liang,*[a] *Ruowen Liang,*[a] *Na Qin,*[a] *Ling Wu*[a,b*]

*a: Research Institute of Photocatalysis, Fujian Provincial Key Laboratory of Photocatalysis--State Key Laboratory Breeding Base, Fuzhou University, Fuzhou 350002, P. R. China*

*b: State Key Laboratory of Structural Chemistry, Fujian Institute of Research on the Structure of Matter, Chinese Academy of Sciences, Fuzhou, Fujian 350002, China*

[*] *Corresponding Author. Tel.: +86 591 83779105; E-mail: wuling@fzu.edu.cn*

**Materials and Reagents.** Zirconium chloride ($ZrCl_4$), and 2-$NH_2$-terephthalic acid ($H_2ATA$) were obtained from Alfa Aesar China Co., Ltd. (Tianjin, China). Potassium dichromate ($K_2Cr_2O_7$), N, N-Dimethylformamide (DMF) and methanol ($CH_3OH$) were supplied by Sinopharm Chemical Reagent Co., Ltd. (Shanghai, China). Graphite powder, sulfuric acid ($H_2SO_4$), nitric acid ($HNO_3$), hydrochloric acid (HCl), potassium persulfate ($K_2S_2O_8$), phosphorus pentoxide ($P_2O_5$), hydrogen peroxide, 30% $H_2O_2$, potassium permanganate ($KMnO_4$), and ethanol ($C_2H_6O$) were obtained from Sinopharm Chemical Reagent Co., Ltd. (Shanghai, China). All materials were used as received without further purification.

**Preparations.** *(a) Synthesis of Zr-2-$NH_2$-benzenedicarboxylate UiO-66($NH_2$).* Sample UiO-66($NH_2$) was synthesized *via* the same procedure as our previous work.[S1] In a typical synthesis, $ZrCl_4$ (0.2332 g, 1.0 mmol) and 2-$NH_2$-benzenedicarboxylate (0.1812 g, 1.0 mmol) were dissolved in DMF (50 mL), and then the solution was transferred to a 100 mL Teflon-lined stainless steel autoclave. The autoclave was sealed and heated in an oven at 120 °C for 48 h under autogenous pressure, after cooled naturally, the sample was purified with anhydrous methanol for several times to make sure that the occluded DMF molecules were eliminated, followed by drying under vacuum (100 °C, 12 h) before using the samples for the photocatalytic reactions.

*(b) Synthesis of Graphene Oxide (GO).* Graphene oxide (GO) was synthesized from natural graphite powder by a modified Hummers method.[S2] In detail, 2 g of graphite powder was put into a mixture of 12 mL of concentrated $H_2SO_4$, 2.5 g of $K_2S_2O_8$, and 2.5 g of $P_2O_5$. The solution was heated to 80 °C in an oil bath kept stirring for 24 h. The mixture was then carefully diluted with 500 mL of deionized (DI) water, filtered, and washed until the pH of rinse water became neutral. The product was dried under ambient condition overnight. This preoxidized graphite was then subjected to oxidation described as follows. In a typical procedure, preoxidized graphite powder was added to a mixture of 120 mL of concentrated $H_2SO_4$ and 30 mL of $HNO_3$ under vigorous stirring, and the solution was cold to 0 °C. Then, 15 g of $KMnO_4$ was added gradually under stirring, and the temperature of the mixture was kept to be below 20 °C by cooling. Then, the mixture was stirred at room temperature for 96 h and diluted with 1 L of DI water in an ice bath to keep the temperature below 50 °C for 2 h. After the further dilution with 1 L of DI water, 20 mL of 30% $H_2O_2$ was then added to the mixture, and a brilliant yellow product was formed along with bubbling. The mixture was filtered and washed with 1:10 HCl aqueous solution to remove metal ions followed by DI water to remove the acid. The filter cake was then dispersed in water by a mechanical agitation. Low-speed centrifugation was done at 1000 rpm for 2 min. The supernatant then underwent two more high-speed centrifugation steps at 8000 rpm for 15 min to remove small GO pieces and

water-soluble byproduct. The final sediment was redispersed in water with mechanical agitation or mild sonication using a table-top ultrasonic cleaner, giving a solution of exfoliated GO. The GO separated and dried is in the form of a brown powder.

*(c) Fabrication of the RGO-UiO-66($NH_2$) NCs.* The GO-UiO-66($NH_2$) was synthesized by electrostatic self-assembly of UiO-66($NH_2$) on the GO: 100 mg UiO-66($NH_2$) was first dispersed in certain amount of water by sonication for 30 min, then a negatively charged GO suspension in water(1 mg·mL$^{-1}$) with the desired weight addition was added to the above dispersion, the weight ratio of GO to UiO-66($NH_2$) NPs is 0:1, 0.01:1, 0.02:1, 0.03:1, 0.05:1 and 0.1:1, respectively, then the above GO-UiO-66($NH_2$) suspension was transferred to a 100 mL Teflon-lined stainless steel autoclave then sealed and heated in an oven at 120 $^{o}$C for 24 h under autogenous pressure for the reduction of GO to RGO. After that, the products were cooled at room temperature and separated by centrifugation and washed, followed by a dry process.

**Characterizations.** Zeta potentials ($\xi$) measurements of the samples were determined by dynamic light scattering analysis (Zeta sizer 3000HSA) at room temperature of 25 °C. In brief, 25 mg of the sample was diluted to 50 mL deionized water to obtain a concentration of ca. 500 mg·L$^{-1}$ in an aqueous solution. The as-prepared samples were characterized by powder X-ray diffraction (XRD) on a Bruker D8 Advance X-ray diffractometer operated at 40 kV and 40 mA with Ni-filtered Cu K$\alpha$ irradiation ($\lambda$ = 1.5406 Å). Transmission electron microscopy (TEM) and high-resolution transmission electron microscopy (HRTEM) images were obtained using a JEOL model JEM2010 EX instrument at an accelerating voltage of 200 kV. UV–vis diffuse reflectance spectra (UV–vis DRS) were obtained by a UV–vis spectrophotometer (Varian Cary 500). Barium sulfate was used as a referent. BET surface area and the $N_2$ adsorption were carried out on an ASAP2020M apparatus (Micromeritics Instrument Corp., USA). After the samples were degassed in vacuum at 120 °C for 6 h, the nitrogen adsorption and desorption isotherms were measured at 77 K. The electrochemical analysis was carried out in a conventional three electrode cell, using a

Pt plate and a saturated Ag/AgCl electrode as counter electrode and reference electrode, respectively. The working electrode was prepared on fluorine-doped tin oxide (FTO) glass, which was cleaned by sonication in deionized water and ethanol for 30 min, and then drying. The FTO slide was dip coated with 10 μL of slurry, which was obtained from the mixture of 5 mg photocatalyst and 0.5 mL $H_2O$ under sonication for 2 h, and the side part of the FTO slide was previously protected using Scotch tape. After air drying naturally, a copper wire was connected to the side part of the FTO glass using a conductive tape. The uncoated parts of the electrode were isolated with an epoxy resin, and the exposed area of the electrode was 0.25 $cm^2$. The working electrodes were immersed in a 0.2 M $Na_2SO_4$ aqueous solution without any additive for 30 s before measurement. The photocurrent measurements were conducted with a BAS Epsilon workstation. A 300 W Xe lamp (Beijing Perfectlight, PLS-SXE 300c) with a 420 nm cut-off filter was used as a light source.

**Evaluation of photocatalytic activity.** Potassium dichromate ($K_2Cr_2O_7$) was chosen as a representative Cr(VI) compound. The photocatalytic reaction was carried out at 30 $^{o}$C in a 100 mL quartz reactor containing 20 mg photocatalyst and 40 mL 10 ppm Cr(VI) aqueous solution. After being stirred for a sufficient amount of time to reach adsorption–desorption equilibrium. The suspensions were irradiated by a 300 W Xe arc lamp (PLS-SXE 300, Beijing Perfectlight Co. Ltd.) with a UV-CUT filter to cut off light of wavelength < 420 nm. During illumination, about 3 mL of suspension was taken from the reactor at a scheduled interval and centrifuged to separate the photocatalyst. The Cr(VI) content in the solution was determined using the diphenylcarbazide (DPC) method.[S3] The Cr(VI) shows a characteristic peak at 540 nm in the UV-vis absorption curve. The higher the Cr(VI) concentration in the solution, the stronger peak intensity was observed. The measured absorbance intensities at different illumination times were transformed to the reduction ratio of Cr(VI), which is calculated using the following expression:

Reduction ratio of Cr(VI) = $(C_0-C_t) / C_0 * 100\%$

Where $C_0$ and $C_t$ are the absorbance intensities when illuminated for 0 (that is, just after the dark adsorption) and $t$ min, respectively.

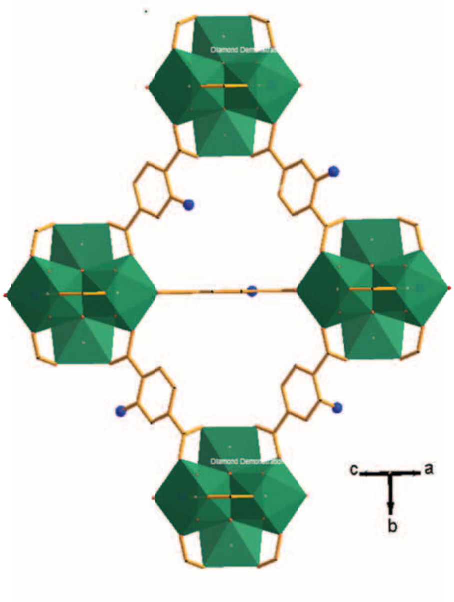

**Fig. S1** A schematic drawing of the structure of UiO-66($NH_2$).

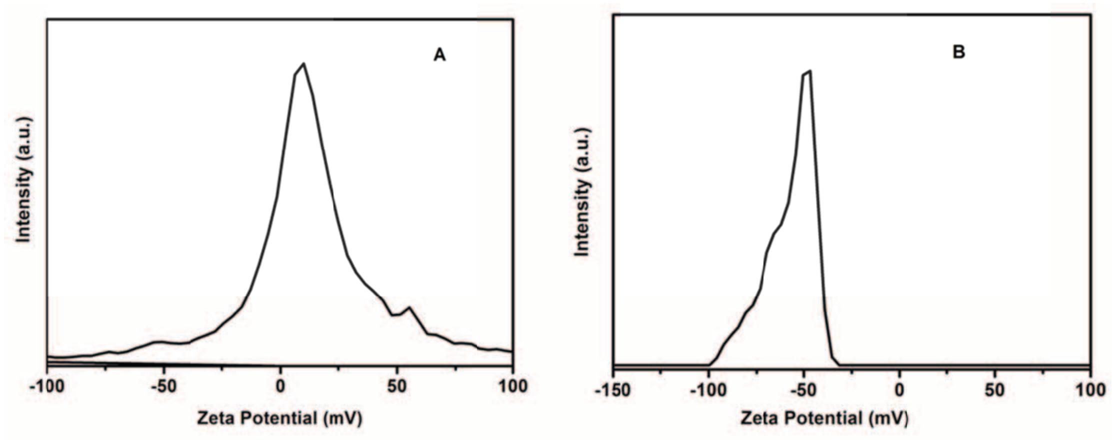

**Fig. S2** The zeta potentials (ξ) of UiO-66($NH_2$) (A) and GO (B) in deionized water without adjusting pH values.

The zeta potential (ξ) measurements have been performed to demonstrate the electrostatic self-assembly process of UiO-66($NH_2$) with GO. Fig. S2 shows ξ values of UiO-66($NH_2$) and GO as a function of pH. As shown in Fig. S2A, the UiO-66($NH_2$) shows a zeta potential value of +9.9 mV when dispersed in water without adding HCl or NaOH aqueous solution, indicating a positively charged surface of UiO-66($NH_2$)

dispersion in water. As shown in Fig. S2B, the zeta potential analysis on the GO colloidal dispersion in water, reveals an obviously negatively charged surface. The negatively charged surface of GO colloids results from the deprotonation of the carboxyl groups (−COOH) during the dialysis process in the synthesis of GO.[S4] Thus, the positively charged UiO-66($NH_2$) and negatively charged GO in water can spontaneously establish a solid basis of electrostatic attraction for the self-assembly construction of the NCs of GO-UiO-66($NH_2$).

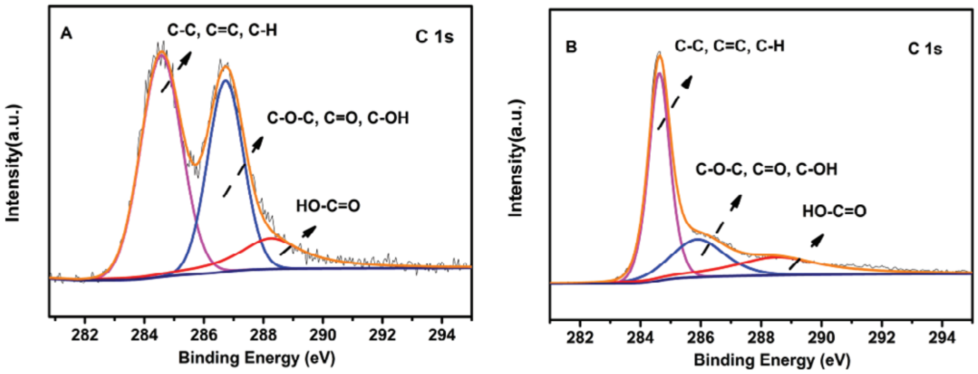

Fig. S3. C 1s X-ray photoelectron spectra (XPS) of original GO (A) and RGO obtained after the hydrothermal reduction (B).

XPS measurements have been carried out to confirm the reduction of GO to RGO. As shown in Fig. S3, for the original GO, the C 1s XPS spectrum suggests the abundance of various oxygen-containing functional groups on the GO surface. For the RGO obtained after the hydrothermal reduction, the significant loss of oxygen-containing functional groups is observed based on the C 1s XPS spectrum, which indicates the efficient reduction of GO to RGO after the hydrothermal reduction treatment.

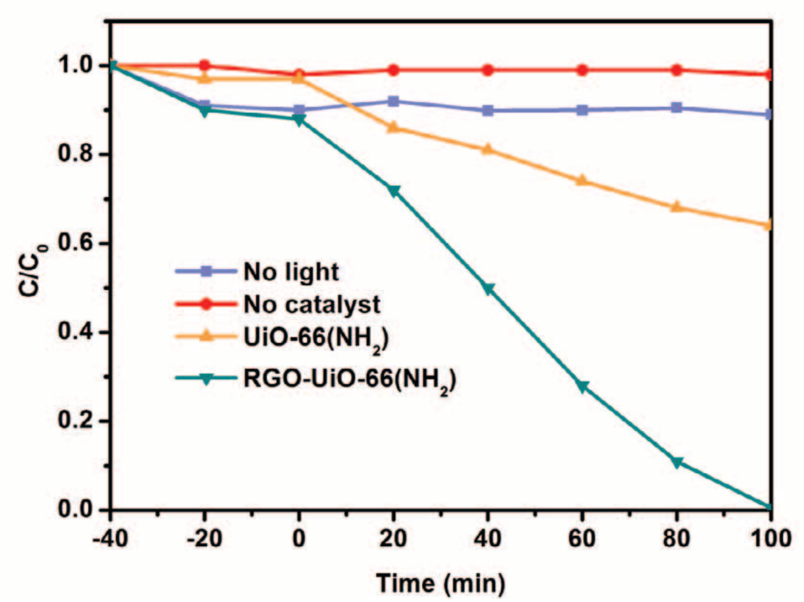

**Fig. S4** Control experiments for the reduction of aqueous Cr(VI) over RGO-UiO-66(NH$_2$) under different conditions. Reaction conditions: 20 mg photocatalyst, 40 mL of 10 ppm Cr(VI), reaction temperature 30 °C, pH=2.

Control experiments show that the reduction of Cr(VI) hardly occurs in the absence of photocatalyst under the same experimental conditions. Furthermore, no reduction of Cr(VI) occurs in the dark, suggesting the photocatalytic nature of the reaction.

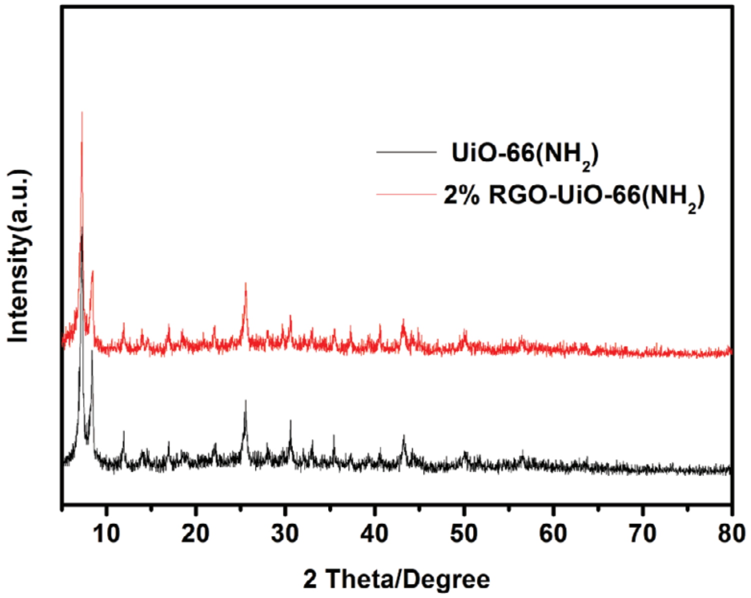

**Fig. S5** XRD patterns of 2% RGO-UiO-66(NH$_2$) before and after the photocatalytic reaction.

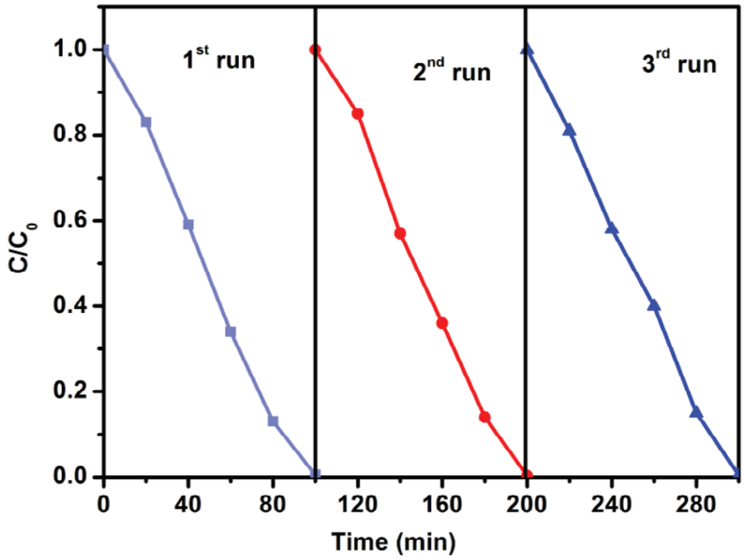

**Fig. S6** Reusability of 2% RGO-UiO-66($NH_2$) for the photocatalytic reduction of Cr(VI).

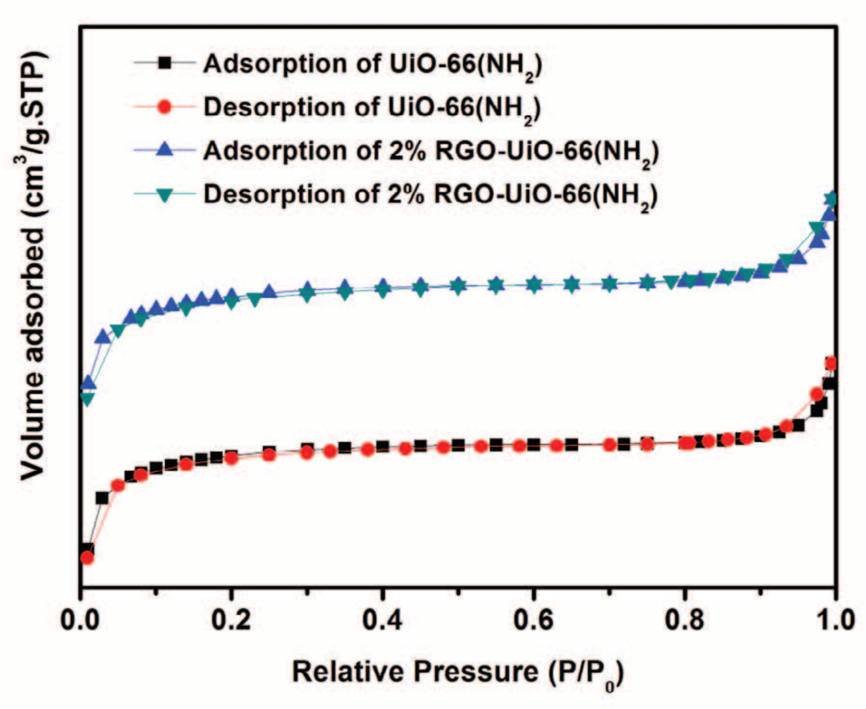

**Fig. S7** BET adsorption-desorption isotherms of UiO-66($NH_2$) (a) and 2%

RGO-UiO-66($NH_2$) (b).

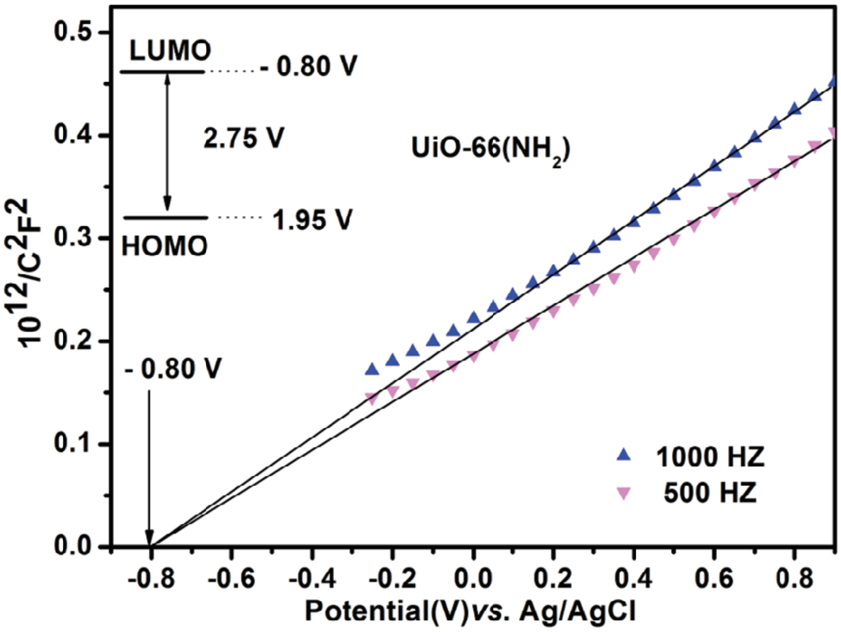

**Fig. S8** Mott-Schottky plot of UiO-66($NH_2$) in 0.2 M $Na_2SO_4$ aqueous solution (pH = 6.8).

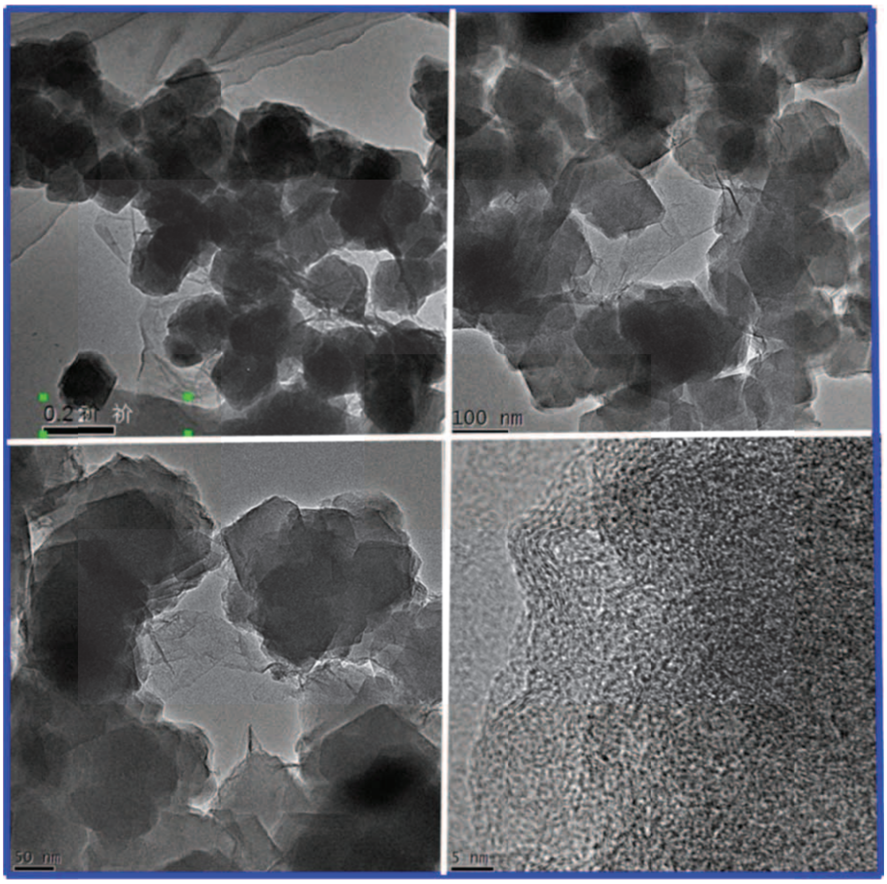

**Fig. S9** TEM and HRTEM images for RGO-UiO-66($NH_2$).

**Table 1S** Summary of surface area, pore volume and pore size of the as-prepared UiO-66($NH_2$) and RGO-UiO-66($NH_2$).

| Sample | $S_{BET}$ ($m^2/g$)$^a$ | Total Pore Volume ($cm^3/g$)$^b$ | ***Avergare pore size (nm)$^c$*** |
|---|---|---|---|
| UiO-66($NH_2$) | 732.21 | 0.089 | 4.11 |
| 1% GR-UiO-66($NH_2$) | 745.67 | 0.091 | 4.08 |
| 2% GR-UiO-66($NH_2$) | 766.54 | 0.095 | 4.09 |
| 3% GR-UiO-66($NH_2$) | 769.51 | 0.101 | 3.99 |
| 5% GR-UiO-66($NH_2$) | 788.51 | 0.14 | 5.11 |
| 10% GR-UiO-66($NH_2$) | 796.45 | 0.20 | 6.88 |

## Equation

$$\text{RGO-UiO-66(NH}_2\text{)} + h\nu \rightarrow \text{RGO-UiO-66(NH}_2\text{)}\ (e^- + h^+) \qquad (1)$$

$$Cr_2O_7^{2-} + 14H^+ + 6e^- \rightarrow 2Cr^{3+} + 7H_2O \qquad (2)$$

$$2H_2O + 4h^+ \rightarrow H_2O_2 + 2H^+ \qquad (3)$$

## Notes and references

S1 L. Shen, S. Liang, W. Wu, R. Liang and L. Wu, *Dalton Trans.,* 2013, **42**, 13649.

S2 W. S. Hummers and R. E.Offeman, *J. Am. Chem. Soc.,* 1958, **80**, 1339.

S3 A. Idris, N. Hassan, R. Rashid and A.-F. Ngomsik, *J. Hazard. Mater.*, 2011, **186**, 629.

S4 (a) D. Li, M. BMuller, SGilje, R. Bkaner and G. G.Wallace, *Nat. Nanotechnol.,* 2008, **3**, 101; (b) T. Szabo, E. Tombacz, E. Illes and I. Dekany, *Carbon,* 2006, **44,** 537; (c) S. Liu and Y-J. Xu, *Nanoscale.,* 2013, **DOI:** 10.1039/C3NR02682E.